DALTON
FULL PAPER

Dinuclear and hexanuclear iron(III) carboxylate clusters with a bis(bipyridine) ligand: supramolecular aggregation of $[Fe_2O_2]$ units to give a $[Fe_6O_6]$ ladder structure †

Elisa J. Seddon,[a] Jae Yoo,[b] Kirsten Folting,[a] John C. Huffman,[a] David N. Hendrickson *[b] and George Christou *[a]

[a] *Department of Chemistry and Molecular Structure Center, Indiana University, Bloomington, IN 47405-7102, USA*
[b] *Department of Chemistry-0358, University of California at San Diego, La Jolla, CA 92093-0358, USA*

Received 20th June 2000, Accepted 7th August 2000
First published as an Advance Article on the web 28th September 2000

The use of the bis-bipyridine ligand L (1,2-bis(2,2′-bipyridyl-6-yl)ethane) in iron(III) chemistry has yielded a variety of new dinuclear and hexanuclear iron complexes, the latter containing a ladder-like supramolecular architecture. Treatment of L with two equivalents of HBF_4 yields $[H_2L][BF_4]_2$ **1**, the doubly protonated ligand. The FeX_3/NaO_2CR/L (2 : 4 : 1) reaction system in MeCN gives $[Fe_2OX_2(O_2CR)_2L]$ (X = Cl, R = Ph **2**; X = Br, R = Ph **3**; X = Cl, R = Me **4**). The same $FeCl_3$/NaO_2CPh/L (2 : 4 : 1) reaction system but in a 1 : 1 MeCN–water solution gives green $[Fe_2OCl_2(O_2CPh)L(H_2O)_2]Cl$ **5**, and in a water solution gives brown $[Fe_6O_6(O_2CPh)_3L_3(H_2O)_2]Cl_3$ **6**. Treatment of a 1 : 2 MeOH–acetone solution of the nitrate salt of **6** with an excess of $NaNO_3$ gives brown-red $[Fe_2O(NO_3)_4L]$ **7**. Reaction of $[NEt_4]_2[Fe_2OCl_6]$ with L and $NaNO_3$ (2 : 2 : 1) in MeCN gives orange-brown $Na_2[Fe_2OCl_6L]$ **8**, whereas reaction with L and NaO_2CPh (1 : 1 : 1) in MeCN gives red-green $[Fe_2OCl_2L_2]Cl_2$ **9**. Complexes **1**, **2** and **5**–**7** were characterized by X-ray crystallography. The cation of **1** exists in a single-step conformation, with planar bpy units stabilized by the presence of intra-bpy hydrogen bonding and intermolecular hydrogen bonding with the anion. All the dinuclear complexes contain a $[Fe_2O]^{4+}$ unit bridged by one L and either zero, one or two carboxylate groups. Complexes **2**–**4** are bridged by two carboxylate groups, with the two terminal halide ligands in a *cis* conformation. Complex **5** contains only one bridging benzoate group, and octahedral geometry at each Fe^{III} is completed with terminal Cl^- and H_2O ligands, with the Cl^- ligands in a *trans* conformation. Complex **6** can be described as three $[Fe_2O_2(O_2CPh)L]^+$ units joined together to give a near-planar $[Fe_6O_6]^{6+}$ ladder-like core. This chain of Fe_2 units is terminated by water molecules. The cation can be prepared as a Cl^-, Br^-, NO_3^-, ClO_4^-, PF_6^-, or BF_4^- salt. Complex **7** contains four chelating NO_3^- ligands and no bridging carboxylate group. Variable-temperature magnetic susceptibility studies of **4** and **6** in the 5.00 to 300 K range reveal both complexes to have $S = 0$ ground states. The data for **4** were fitted by the appropriate theoretical expression for a Fe^{III}_2 complex and a molar fraction (p) of $S = 5/2$ paramagnetic impurity, giving $J = -119$ (1.5) cm^{-1}, $g = 1.96(2)$ and $p = 0.0102(2)$, with temperature-independent paramagnetism held constant at 500×10^{-6} cm^3 mol^{-1}. The obtained J value is consistent with that predicted by a previously published magnetostructural relationship.

Introduction

In the last several years we have been very interested in developing 3d metal coordination cluster chemistry with oxide bridges and predominantly carboxylate peripheral ligation. These efforts have usually also involved the use of a chelating ligand such as 2,2′-bipyridine (bpy), 2-picolinate (pyridine-2-carboxylate) (pic^-) or the anion of dibenzoylmethane (dbm^-). The presence of a chelating ligand was found to have profound effects on the nuclearity and metal topology of the resultant product.[1] Thus, for example, the reaction of bpy with $[Mn_3O(O_2CR)_6(py)_3]^+$ was the original way by which the tetranuclear butterfly complexes $[Mn_4O_2(O_2CR)_7(bpy)_2]^+$ were obtained.[2]

Another area in which ligands involving multiple 2,2′-bipyridine units such as oligo-pyridine and -bipyridine ligands have been employed is the exploding area of supramolecular chemistry. This strategy has commonly been employed by several groups for the synthesis of a variety of complexes with multiple mononuclear metal centers, and fascinating supramolecular architectures such as helices, grids, ladders, cages, *etc*. have been described.[3] The choice of ligand in such studies is obviously crucial, because the hapticity, flexibility, chelate bite size(s) and other ligand properties are of paramount importance in determining the structure of the product.

Very recently we began a program that can be considered a hybrid of the above two approaches. We have been exploring the use in cluster chemistry of the type of ligands that have been employed to date in supramolecular chemistry with mononuclear metal units. Our belief was that such ligands could provide access to new types of clusters and/or supramolecular architectures involving repeating cluster units rather than repeating mononuclear centers. Initial work has concentrated on the use of the bis(bipyridine) ligand L (1,2-bis(2,2′-bipyridyl-6-yl)ethane)[4] and has proved the feasibility of this approach by providing us with novel 3d metal cluster types such as the face-sharing triple cubane core of $[Co_8O_4(OH)_4(O_2CMe)_6L_2]^{2+}$,[5] the "dimer-of-dimers" topology of $[Mn_4O_2(O_2CMe)_4L_2]^{2+}$ [6] and the 'four-rung ladder' core of $[Fe_6O_4Cl_4(O_2CPh)_4L_2]^{2+}$.[7] In this paper, we report the extension of our studies with L in iron(III)

† Electronic supplementary information (ESI) available: rotatable 3-D crystal structure diagram in CHIME format. See http://www.rsc.org/suppdata/dt/b0/b004925p/

 DOI: 10.1039/b004925p

cluster chemistry, including the preparation and properties of dinuclear units and a new 'six-rung ladder' core in $[Fe_6O_6(O_2CPh)_3(H_2O)_2L_3]^{3+}$.

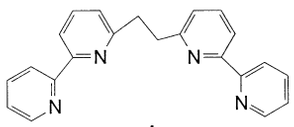

L

Experimental

Syntheses

All manipulations were carried out under aerobic conditions using materials as received. $[NEt_4]_2[Fe_2OCl_6]$[8] and the bis-bipyridine ligand L[4] were prepared as described elsewhere.

$[H_2L][BF_4]_2$ 1. L (0.20 g, 0.60 mmol) was dissolved in hot MeOH (75 mL) and treated with $HBF_4{\cdot}Et_2O$ (85%, 205 μL, 1.2 mmol). The solvent was removed *in vacuo* and the white solid recrystallized from a MeCN–Et_2O solvent layering to give white crystals in 38% yield. Calc. (Found) for $C_{24}H_{25}B_2F_8N_4O_{0.5}$ (**1**·0.5Et_2O): C, 52.31 (52.58); H, 4.57 (4.27); N, 10.17 (10.45)%. ^{1}H NMR (400 MHz, CD_3CN): δ 8.77 (d, 1 H), 8.57 (m, 2 H), 8.21 (d, 1 H), 8.12 (t, 1 H), 7.98 (m, 1 H), 7.67 (d, 1 H) [aromatic], 4.05 (broad NH) and 3.61 (s, 4 H, CH_2). ^{13}C NMR (400 MHz, CD_3CN): δ 161.88, 148.04, 147.52, 146.19, 144.38, 142.32, 128.65, 128.52, 125.02, 121.99 and 36.10.

$[Fe_2OCl_2(O_2CPh)_2L]$ 2. *Method 1.* Anhydrous $FeCl_3$ (0.18 g, 1.1 mmol), NaO_2CPh (0.32 g, 2.2 mmol) and L (0.19 g, 0.55 mmol) were dissolved in MeCN (50 mL) and the solution refluxed overnight. The NaCl was removed by filtration, and the filtrate stored at 5 °C for 10 d to give a green crystalline solid. This was collected by filtration and recrystallized from boiling MeCN. Storage of the flask at 5 °C for 4 d gave dark green crystals that were filtered off and washed with a little ice-cold MeCN. The yield was 94 mg (22%). The crystals turn to powder on drying; a vacuum-dried sample analysed as **2**·MeCN·H_2O. Calc. (Found) for $C_{38}H_{33}Cl_2Fe_2N_5O_6$: C, 54.44 (54.30); H, 3.97 (3.90); N, 8.35 (8.23%). Selected IR data (cm^{-1}): 1624w, 1599m, 1545m, 1455m, 1393s, 781m, 722m, 673w, 641w and 540w (br).

Method 2. $[NEt_4]_2[Fe_2OCl_6]$ (0.18 g, 0.30 mmol), NaO_2CPh (0.088 g, 0.60 mmol) and L (0.10 g, 0.30 mmol) were dissolved in MeCN (50 mL), the solution refluxed overnight, filtered, and the filtrate maintained at 5 °C for 7 d. A small amount of powder was removed by filtration, and the filtrate maintained at 5 °C for 14 d. This gave large dark green crystals in 11% yield, which were filtered off, washed with a little ice-cold MeCN and dried *in vacuo*. IR examination confirmed this product to be complex **2**.

$[Fe_2OBr_2(O_2CPh)_2L]$ 3. Anhydrous $FeBr_3$ (0.18 g, 0.60 mmol), NaO_2CPh (0.180 g, 1.12 mmol) and L (0.10 g, 0.30 mmol) were dissolved in MeCN (20 mL). After 3 d at room temperature the resultant light brown precipitate was collected by filtration, washed with a little ice-cold water and then THF, and dried *in vacuo*. The yield was 0.25 g (95%). Calc. (Found) for $C_{36}H_{32}Br_2Fe_2N_4O_7$ (**3**·2H_2O): C, 47.82 (49.79); H, 3.57 (3.36); N, 6.20 (6.09)%.

$[Fe_2OCl_2(O_2CMe)_2L]$ 4. A solution of anhydrous $FeCl_3$ (0.202 g, 1.25 mmol), NaO_2CMe (0.205 g, 2.50 mmol) and L (0.21 g, 0.63 mmol) in MeCN (50 mL) was refluxed overnight. After removing NaCl and a chocolate brown powder by filtration, the brown filtrate was layered with Et_2O. After 4 d, 0.15 mg (33% yield) of dark green crystals was collected by filtration from a dark brown solution and rinsed with a small amount of ice-cold MeCN. A vacuum-dried sample analysed for **4**·$\frac{3}{4}$MeCN. Calc. (Found) for $C_{27.5}H_{26.25}Cl_2Fe_2N_{4.75}O_5$: C, 48.16 (48.06); H, 3.86 (3.60); N, 9.70 (9.77)%.

$[Fe_2OCl_2(O_2CPh)L(H_2O)_2]Cl$ 5. A solution of anhydrous $FeCl_3$ (92 mg, 0.57 mmol) in a solvent mixture of MeCN (30 mL) and water (5 mL) was treated with NaO_2CPh (0.16 g, 1.1 mmol) and L (96 mg, 0.28 mmol), followed by the addition of more water (25 mL). The solution was stirred overnight, filtered to remove a small amount of brown powder from the light brown solution, and the solvent removed under vacuum. The residue was dissolved in a mixture of MeCN (5 mL) and water (0.5 mL) and layered with Et_2O. Large green rhombohedral crystals of complex **5**·2MeCN·2H_2O formed on the sides of the tube in small yield. A small amount of **2** formed on the bottom and was removed by pipette (identified spectroscopically). The remaining crystals were collected by filtration, washed with Et_2O and dried under vacuum. Dried solid analysed as solvent-free. Calc. (Found) for $C_{29}H_{27}Cl_3Fe_2N_4O_5$: C, 47.74 (48.03); H, 3.73 (3.37); N, 7.68 (7.87)%. Selected IR data (cm^{-1}): 1640w (br), 1597m, 1562w, 1507m, 1489w, 1453s, 1408s, 1399s, 837m, 781s, 721m, 677w, 642w, 540w (br), 476w and 438w.

$[Fe_6O_6(O_2CPh)_3L_3(H_2O)_2]Cl_3$ 6. A solution of anhydrous $FeCl_3$ (0.19 g, 1.2 mmol), NaO_2CPh (0.34 g, 2.4 mmol) and L (0.20 g, 0.60 mmol) in water (50 mL) was stirred overnight and filtered to remove a tan solid (containing Fe and $PhCO_2^-$, but no L, by IR examination). The brown filtrate was treated with NaCl (1.5 g, 26 mmol) and maintained at room temperature for 3 d to give dark brown crystals. These were collected by filtration and dried *in vacuo*. The yield was 0.063 g (19%). Dried solid analysed as **6**·6H_2O. Calc. (Found) for $C_{87}H_{85}Cl_3Fe_6N_{12}O_{20}$: C, 50.72 (50.66); H, 4.16 (3.96); N, 8.16 (7.96)%. [The crystallographic sample was prepared by adding an excess of NMe_4Cl (0.24 g) to 5.0 mL of a 0.4 M aqueous solution of **6**·6H_2O and maintaining the solution at room temperature for one week: this was identified crystallographically as **6**·19H_2O.] Selected IR data (cm^{-1}): 1697w (br), 1630w (br), 1599m, 1572w, 1491w, 1453m, 1400s, 781m, 720m, 685w, 654w, 641m and 463m.

The corresponding Br^- salt was prepared in an analogous manner using $FeBr_3$, or by using $FeCl_3$ and treating the filtrate with an excess of NaBr instead of NaCl. The NO_3^-, ClO_4^-, PF_6^- and BF_4^- salts could be made in an analogous manner.

$[Fe_2O(NO_3)_4L]$ 7. *Method 1.* A concentrated solution of complex **6** in MeOH was diluted with two volumes of acetone and the solution maintained at room temperature for one week to give brown-red needles suitable for crystallography.

Method 2. A solution of $Fe(NO_3)_3{\cdot}9H_2O$ (0.25 g, 0.60 mmol) and L (0.10 g, 0.30 mmol) in MeOH (50 mL) was gently warmed for 2 h during which time a dirty green powder precipitated. This was filtered off, washed with MeOH and dried *in vacuo*. The yield was 165 mg (77%).

$Na_2[Fe_2OCl_6L]$ 8. A solution of $[NEt_4]_2[Fe_2OCl_6]$ (0.18 g, 0.30 mmol) in MeCN (20 mL) was treated with L (0.10 g, 0.30 mmol) and $NaNO_3$ (0.11 g, 0.12 mmol) and stirred overnight in a sealed flask. A fine orange-brown powder was removed by decantation from a heavy solid, which was then collected by filtration, washed with MeCN and dried *in vacuo*. The yield was 0.11 g (52%). Calc. (Found) for $C_{22}H_{18}Fe_2Cl_6N_4Na_2O$: C, 36.46 (36.82); H, 2.50 (2.46); N, 7.73 (7.68)%.

$[Fe_2OCl_2L_2]Cl_2$ 9. A solution of $[NEt_4]_2[Fe_2OCl_6]$ (0.098 g, 0.16 mmol) in MeCN (10 mL) was treated with NaO_2CPh (0.023 g, 0.16 mmol) and L (0.058 g, 0.17 mmol) and the red-brown solution stirred for 1 h, filtered, and the filtrate layered with Et_2O. After one week a mixture of pink powder and

red-green dichroic crystals were collected and separated from each other by decantation; their IR spectra were identical. Vacuum-dried solid analysed as **9**·H_2O. Calc. (Found) for $C_{22}H_{19}Cl_2FeN_4O$: C, 54.80 (54.85); H, 3.97 (4.04); N, 11.62 (11.41)%.

X-Ray crystallography

Data were collected using a Picker four-circle diffractometer or a Bruker SMART CCD diffractometer. The structures were solved by direct methods (MULTAN[9a] or SHELXTL[9b]) and standard Fourier techniques and refined on *F* by full-matrix least-squares cycles. Data collection, unit cell parameters, and structure refinement details are listed in Table 1.

CCDC reference number 186/2139.

See http://www.rsc.org/suppdata/dt/b0/b004925p/ for crystallographic files in .cif format.

Physical measurements

IR and electronic spectra were recorded on KBr pellets and solutions on Nicolet Model 510P and Hewlett Packard Model 8452A spectrophotometers, respectively. DC magnetic susceptibility data were collected on powdered, microcrystalline samples (restrained in eicosane to prevent torquing) on a Quantum Design MPMS5 SQUID magnetometer equipped with a 5.5 T (55 kG) magnet. A diamagnetic correction to the observed susceptibilities was applied using Pascal's constants.

Results and discussion

Syntheses

Our previous investigation of the use of the bis-bipyridine ligand L in iron(III) carboxylate chemistry led to the isolation of $[Fe_6O_4Cl_4(O_2CPh)_4L_2][FeCl_4]_2$ and $[Fe_2(OMe)_2Cl_2(O_2CPh)L][FeCl_4]$.[7] The latter contains a $[Fe_2(\mu\text{-}OMe)_2]^{4+}$ core, whereas the former contains a cation with a $[Fe_4(\mu_3\text{-}O)_4]^{4+}$ "four-rung ladder" core, the ladder terminated by two additional Fe atoms, as shown below. These two complexes were obtained using the

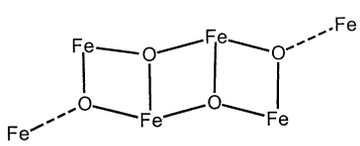

$FeCl_3$: NaO_2CPh : L reaction system in MeCN (4 : 4 : 1) and MeOH (3 : 3 : 1), repectively.[7] More recently, use of the same reaction system but employing a 2 : 4 : 1 ratio and changing the solvent and/or source of iron has allowed access to a variety of new products with interesting structures. The 2 : 4 : 1 reaction in MeCN gave a solution from which crystallized $[Fe_2OCl_2(O_2CPh)_2L]$·2.5 MeCN (**2**·2.5 MeCN) in 22% yield upon standing for 4 days at 5 °C. This is summarized in eqn. (1),

$$2\ FeX_3 + 4\ NaO_2CR + L + H_2O \longrightarrow [Fe_2OX_2(O_2CR)_2L] + 4\ NaX + 2\ HO_2CR \quad (1)$$

which assumes that adventitious water is the source of the O^{2-} ion. When X = Br and R = Ph, $[Fe_2OBr_2(O_2CPh)_2L]$ **3** precipitates from solution as a light brown powder in near quantitative yield. When X = Cl and R = Me, crystalline $[Fe_2OCl_2(O_2CMe)_2L]$ **4** is obtained in 33% yield after standing for 4 days at 5 °C.

Changing the reaction solvent greatly influences the nature of the product. A different dinuclear complex is obtained from the 2 : 4 : 1 ratio in MeCN when water is slowly added to achieve a 1 : 1 water–MeCN solvent composition; solvent removal and recrystallization from a MeCN–Et_2O solvent layering gave $[Fe_2OCl_2(O_2CPh)L(H_2O)_2]Cl$ **5** in low yield. This reaction is summarized in eqn. (2). The excess of NaO_2CPh is beneficial to

$$2\ FeCl_3 + 4\ NaO_2CPh + L + 3\ H_2O \longrightarrow [Fe_2OCl_2(O_2CPh)L(H_2O)_2]Cl + 3\ NaCl + 2\ HO_2CPh + NaO_2CPh \quad (2)$$

the preparation; use of the stoichiometric amount of NaO_2CPh (a 2 : 3 : 1 reaction ratio) does not give pure complex **5**; instead, a large amount of light brown powder precipitates from solution and this material has proven difficult to characterize.

In a completely aqueous reaction solution the product is again different. The reaction utilizing a 2 : 4 : 1 ratio in distilled water gives a tan by-product (containing no L), which can be separated from a dark brown solution by filtration. Addition of NaCl to the filtrate gives crystalline $[Fe_6O_6(O_2CPh)_3L_3(H_2O)_2]Cl_3$ **6** in 19% yield. Its formation is summarized in eqn. (3). Increasing the quantity of $PhCO_2^-$ to the stoichiometric amount (2 : 5 : 1) needed to sequester all H^+ increases the amount of by-product rather than increasing the yield of product.

$$6\ FeCl_3 + 12\ NaO_2CPh + 3\ L + 8\ H_2O \longrightarrow [Fe_6O_6(O_2CPh)_3L_3(H_2O)_2]Cl_3 + 12\ NaCl + 9\ HO_2CPh + 3\ H^+ + 3\ Cl^- \quad (3)$$

As previously noted, the 3 : 3 : 1 ratio in MeOH gives $[Fe_2(OMe)_2Cl_2(O_2CPh)L][FeCl_4]$.[7] When $Fe(NO_3)_3$·$9H_2O$ is treated with L in hot MeOH in a 2 : 1 ratio $[Fe_2O(NO_3)_4L]$ **7** is the product that precipitates from solution, regardless of the presence or absence of carboxylate. Its formation is summarized in eqn. (4). Complex **7** can also be obtained by dissolving

$$2\ Fe(NO_3)_3 + L + H_2O \longrightarrow [Fe_2O(NO_3)_4L] + 2\ HNO_3 \quad (4)$$

$[Fe_6O_6(O_2CPh)_3L_3(H_2O)_2][NO_3]_3$ (the nitrate salt of **6**) in MeOH and diluting with acetone. Even though there is ample opportunity for incorporation of MeO^- or $PhCO_2^-$ into the product, this is not observed. An excess of $NaNO_3$ is beneficial to the formation of **7**, as summarized in eqn. (5).

$$[Fe_6O_6(O_2CPh)_3L_3(H_2O)_2][NO_3]_3 + 3\ H_2O + 9\ NaNO_3 \longrightarrow 3\ [Fe_2O(NO_3)_4L] + 3\ NaO_2CPh + 6\ NaOH \quad (5)$$

In contrast, directed attempts to obtain complex **7** from treatment of $[NEt_4]_2[Fe_2OCl_6]$ with L and $NaNO_3$ in MeCN resulted instead in the formation of $Na_2[Fe_2OCl_6L]$ **8** in 52% yield, eqn. (6). This is probably due to the low solubility of **8** in

$$[NEt_4]_2[Fe_2OCl_6] + L + 2\ NaNO_3 \longrightarrow Na_2[Fe_2OCl_6L] + 2\ NEt_4NO_3 \quad (6)$$

MeCN, because several species are likely present in this reaction solution. Use of $NaBF_4$ instead of $NaNO_3$ also gives complex **8** and in comparable yield. Similarly, an attempt to obtain **5** in a rational manner by treating $[NEt_4]_2[Fe_2OCl_6]$ with L and NaO_2CPh in MeCN resulted instead in the formation of $[Fe_2OCl_2L_2]Cl_2$ **9**, eqn. (7).

$$[NEt_4]_2[Fe_2OCl_6] + 2\ L + 2\ NaO_2CPh \longrightarrow [Fe_2OCl_2L_2]Cl_2 + 2\ NaCl + 2\ NEt_4O_2CPh \quad (7)$$

Crystal structures

ORTEP[9d] representations of complexes **1**, **2**, and **7** and the cations of **5** and **6** are provided in Figs. 1–6, and selected interatomic distances and angles are listed in Tables 2–6.

Salt **1** crystallizes in centrosymmetric space group $P\bar{1}$ with the doubly protonated ligand L lying on a center of inversion (Fig. 1). The cation is in a single-step conformation, where the parallel planes formed by the bipyridine rings are offset by 1.38 Å as a result of the CH_2CH_2 linker. The pyridine N atoms are

Table 1 Crystallographic data for compounds **1**, **2**·2.5MeCN, **5**·2H_2O·2MeCN, **6**·19H_2O and **7**

	1	**2**	**5**	**6**	**7**
Formula[a]	$C_{22}H_{20}B_2F_8N_4$	$C_{41}H_{35.5}Cl_2Fe_2N_{6.5}O_5$	$C_{33}H_{37}Cl_3Fe_2N_6O_7$	$C_{87}H_{111}Cl_3Fe_6N_{12}O_{33}$	$C_{22}H_{18}Fe_2N_8O_{13}$
Formula weight/g mol^{-1}	514.04	881.87	847.75	2294.34	714.13
Space group	$P\bar{1}$	$P\bar{1}$	$C2/c$	$P\bar{1}$	$P2_1/c$
a/Å	9.341(7)	11.459(6)	14.343(8)	18.272(3)	8.759(2)
b/Å	11.460(4)	16.457(8)	17.631(10)	20.688(3)	18.811(6)
c/Å	5.383(6)	11.376(6)	14.465(8)	15.284(2)	16.618(5)
α/°	95.73(9)	92.36(3)		102.50(1)	
β/°	105.82(10)	105.11(3)	90.12(3)	95.01(1)	104.75(1)
γ/°	90.06(5)	74.40(3)		101.05(1)	
V/Å^3	551(2)	1994(2)	3658(2)	5486(2)	2648(2)
Z	1	2	4	2	4
T/°C	−100	−165	−169	−168	−166
λ/Å[b]	0.71069	0.71069	0.71069	0.71069	0.71069
μ/cm^{-1}	1.394	9.139	10.664	9.233	11.808
No. measured/observed reflections	1943/1016	7057/5457	3221/2302	19353/11187	4689/3121
R (R_w) (%)	7.07 (7.19)	4.48 (4.57)	6.75 (5.73)	9.45 (10.34)	4.83 (4.76)

[a] Including solvate molecules. [b] Graphite monochromator.

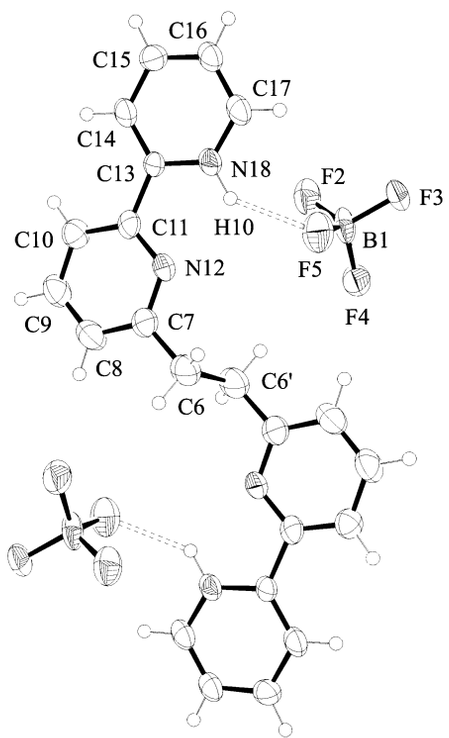

Fig. 1 ORTEP representation at the 50% probability level of $[H_2L][BF_4]_2$ **1** showing N–H · · · F hydrogen bonds as dashed lines.

cis within a bpy unit, and the two bpy units are *anti* about the CH_2CH_2 linker, similar to $[H_2qpy][PF_6]_2$ (qpy = quinquepyridine)[10] and [Hterpy][F_3CSO_3].[11] Each bpy unit is essentially planar with a N8–C13–C11–N12 torsion angle of 4.3°. This *cis* arrangement is undoubtedly stabilized by the presence of intra-bpy hydrogen bonding; although the proton has not directly been located, the presence of a short contact with the BF_4^- anion indicates an intermolecular F5 · · · H–N18 hydrogen bond [N18 · · · F5 2.888(8) and N12 · · · F5 3.561(8) Å]. There is likely a weak N18–H · · · N12 hydrogen bond keeping the bpy unit planar and *cis*.

The neutral ligand L has not crystallographically been characterized, although there are many crystal structures for bipyridine and its derivatives,[12] and for polypyridinium compounds with a variety of anions.[10,11,13] It is interesting that the majority of crystallographically characterized polypyridinium compounds exhibit similar intramolecular/intermolecular hydrogen bonds as in salt **1**, where the proton is simultaneously interacting with two pyridine nitrogen atoms and an atom from the anion.

Table 2 Selected bond distances (Å) and angles (°) for $[H_2L][BF_4]_2$ **1**[a]

N(12)–C(7)	1.337(7)	C(10)–C(11)	1.374(7)
N(12)–C(11)	1.331(7)	C(11)–C(13)	1.492(7)
N(18)–C(13)	1.351(6)	C(13)–C(14)	1.366(8)
N(18)–C(17)	1.349(6)	C(14)–C(15)	1.396(8)
C(6)–C(6′)	1.497(10)	C(15)–C(16)	1.380(8)
C(6)–C(7)	1.509(9)	C(16)–C(17)	1.362(8)
C(7)–C(8)	1.388(8)	N(18) · · · F(5)	2.888(8)
C(8)–C(9)	1.372(9)	N(18)–H(10)	1.09(2)
C(9)–C(10)	1.393(8)	N(12) · · · F(5)	3.561(8)
C(7)–N(12)–C(11)	118.5(5)	N(12)–C(11)–C(13)	113.7(4)
C(13)–N(18)–C(17)	122.9(5)	C(10)–C(11)–C(13)	122.2(5)
C(6′)–C(6)–C(7)	111.7(7)	N(18)–C(13)–C(11)	115.1(5)
N(12)–C(7)–C(6)	116.1(5)	N(18)–C(13)–C(14)	118.3(5)
N(12)–C(7)–C(8)	121.2(6)	C(11)–C(13)–C(14)	126.5(5)
C(6)–C(7)–C(8)	122.7(5)	C(13)–C(14)–C(15)	120.4(5)
C(7)–C(8)–C(9)	119.7(6)	C(14)–C(15)–C(16)	119.2(6)
C(8)–C(9)–C(10)	119.2(5)	C(15)–C(16)–C(17)	119.5(5)
C(9)–C(10)–C(11)	117.2(6)	N(18)–C(17)–C(16)	119.8(5)
N(12)–C(11)–C(10)	124.1(5)		

[a] N(18) and its symmetry-related partner are the protonated atoms.

Complex **2** crystallizes in centrosymmetric space group $P\bar{1}$. The neutral molecule contains a $[Fe_2O]^{4+}$ core bridged by one L and two $PhCO_2^-$ groups, with octahedral geometry at each Fe^{III} completed with terminal Cl^- ions (Fig. 2). The Fe · · · Fe distance of 3.1659(13) Å is typical for dinuclear species with one oxo and two carboxylate bridges;[14] for example, the Fe · · · Fe distance in the analogous $[Fe_2OCl_2(O_2CMe)_2(bpy)_2]$ is 3.151(1) Å,[15] and in the closely related $[Fe_2O(mpdp)(4,4'\text{-}Me_2bpy)_2Cl_2]$ (mpdp = *m*-phenylenedipropionate) it is 3.130(1) Å.[16] The terminal Cl^- ligands are in a *cis* arrangement with a C13–Fe2–Fe1–C14 torsion angle of 14.3°, in contrast to $[Fe_2O(mpdp)(4,4'\text{-}Me_2bpy)_2Cl_2]$ with a torsion angle of 82.3° and $[Fe_2OCl_2(O_2CMe)_2(bpy)_2]$ where the Cl^- ligands are *trans*. The nearly eclipsed arrangement of the Fe–Cl groups in **2** reflects the restricted flexibility of the L ligand, and the bottom view in Fig. 2 shows that the L ligand is distinctly distorted like a bow compared with **1**, and it is clear that an increase in the Cl–Fe–Fe–Cl torsion angle would strain the L group further. Further, it does not appear possible for L to adopt a planar conformation as in **1** in the presence of the $[Fe_2(\mu\text{-}O)(\mu\text{-}O_2CR)_2]$ core which takes up three facial sites at each metal ion.

Complex **5** crystallizes in monoclinic space group $C2/c$. The cation of **5** contains a single oxide bridge as in **2**, but is additionally bridged by one L and only *one* $PhCO_2^-$ group, with terminal Cl^- and H_2O ligands completing octahedral geometry

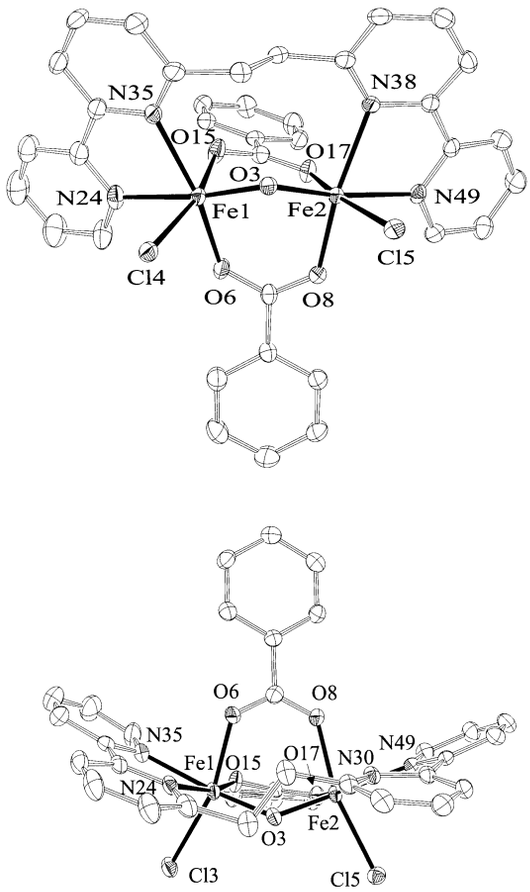

Fig. 2 ORTEP representation at the 50% probability level of $[Fe_2OCl_2(O_2CPh)_2L]$ **2** from two approximately perpendicular viewpoints to emphasize the bowing of the L ligand.

Table 3 Selected bond distances (Å) and angles (°) for $[Fe_2OCl_2(O_2CPh)_2L]$ **2**

Fe(1)···Fe(2)	3.1659(13)	Fe(2)–Cl(5)	2.3806(16)
Fe(1)–Cl(4)	2.3658(15)	Fe(2)–O(3)	1.7813(24)
Fe(1)–O(3)	1.7750(26)	Fe(2)–O(8)	2.0340(26)
Fe(1)–O(6)	2.0630(27)	Fe(2)–O(17)	2.0847(27)
Fe(1)–O(15)	2.0701(27)	Fe(2)–N(38)	2.246(3)
Fe(1)–N(24)	2.169(3)	Fe(2)–N(49)	2.174(3)
Fe(1)–N(35)	2.233(3)		
Cl(4)–Fe(1)–O(3)	99.70(9)	O(15)–Fe(1)–N(35)	84.40(11)
Cl(4)–Fe(1)–O(6)	93.19(9)	N(24)–Fe(1)–N(35)	75.55(12)
Cl(4)–Fe(1)–O(15)	164.90(8)	Cl(5)–Fe(2)–O(3)	95.70(9)
Cl(4)–Fe(1)–N(24)	86.45(9)	Cl(5)–Fe(2)–O(8)	95.09(8)
Cl(4)–Fe(1)–N(35)	90.54(9)	Cl(5)–Fe(2)–O(17)	166.05(7)
O(3)–Fe(1)–O(6)	95.20(11)	Cl(5)–Fe(2)–N(38)	90.20(9)
O(3)–Fe(1)–O(15)	95.14(12)	Cl(5)–Fe(2)–N(49)	84.80(8)
O(3)–Fe(1)–N(24)	171.79(12)	O(3)–Fe(2)–O(8)	95.95(11)
O(3)–Fe(1)–N(35)	98.81(12)	O(3)–Fe(2)–O(17)	98.25(11)
O(6)–Fe(1)–O(15)	88.22(11)	O(3)–Fe(2)–N(38)	96.94(12)
O(6)–Fe(1)–N(24)	89.85(12)	O(3)–Fe(2)–N(49)	171.68(11)
O(6)–Fe(1)–N(35)	164.68(11)	O(8)–Fe(2)–O(17)	83.64(11)
O(15)–Fe(1)–N(24)	78.51(12)	O(8)–Fe(2)–N(38)	165.51(11)
O(8)–Fe(2)–N(49)	92.28(11)	N(38)–Fe(2)–N(49)	74.74(12)
O(17)–Fe(2)–N(38)	87.98(11)	Fe(1)–O(3)–Fe(2)	125.80(14)
O(17)–Fe(2)–N(49)	81.38(10)		

at each Fe^{III} (Fig. 3). The Fe···Fe distance of 3.248(2) Å in this complex is longer than in **2** (3.1659(13) Å), as expected from the change of bridging ligands. This extra degree of freedom allows a perfectly *trans* arrangement of the Cl^- ligands with a Cl2–Fe1–Fe1′–Cl2′ torsion angle of 181.7°. Similarly, the L ligand is nearly planar with a conformation much more like that in **1** than **2** (Fig. 3, bottom). There is no bpy analog for this complex; however, a similar $[Fe_2O(O_2CR)]^{3+}$ core

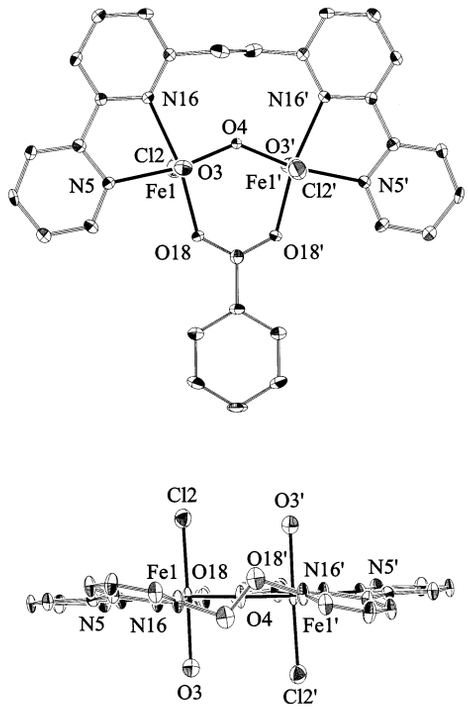

Fig. 3 ORTEP representation at the 50% probability level of the $[Fe_2OCl_2(O_2CPh)L(H_2O)_2]^+$ cation of complex **5** from two viewpoints to emphasize the near planarity of the L ligand.

Table 4 Selected bond distances (Å) and angles (°) for $[Fe_2OCl_2(O_2CPh)L(H_2O)_2]Cl$ **5**[a]

Fe(1)···Fe(1)′	3.248(2)	Fe(1)–O(18)	2.016(4)
Fe(1)–Cl(2)	2.367(2)	Fe(1)–N(5)	2.123(5)
Fe(1)–O(3)	2.158(4)	Fe(1)–N(16)	2.207(4)
Fe(1)–O(4)	1.761(2)		
Cl(2)–Fe(1)–O(3)	178.69(12)	O(3)–Fe(1)–N(16)	87.01(17)
Cl(2)–Fe(1)–O(4)	93.50(6)	O(4)–Fe(1)–O(18)	98.39(19)
Cl(2)–Fe(1)–O(18)	92.95(13)	O(4)–Fe(1)–N(5)	168.45(19)
Cl(2)–Fe(1)–N(5)	89.82(14)	O(4)–Fe(1)–N(16)	92.26(19)
Cl(2)–Fe(1)–N(16)	92.64(14)	O(18)–Fe(1)–N(5)	92.47(16)
O(3)–Fe(1)–O(4)	87.78(12)	O(18)–Fe(1)–N(16)	167.64(17)
O(3)–Fe(1)–O(18)	87.15(16)	N(5)–Fe(1)–N(16)	76.53(17)
O(3)–Fe(1)–N(5)	88.87(17)	Fe(1)–O(4)–Fe(1)′	134.5(3)

[a] Primed atoms are related by a twofold axis to their unprimed partner.

appears in a number of complexes where a tetradentate ligand is coordinated to each Fe^{III}.[17,18] In contrast to these other complexes, the bridging mode of L in **5** shortens the Fe···Fe distance; for example, in $[Fe_2O(O_2CMe)L'_2]ClO_4$ (where L′ is a tetradentate chelating ligand), the Fe···Fe distance is 3.564(2) Å,[18] much longer than in complex **5**.

Complex **6** crystallizes in centrosymmetric space group $P\bar{1}$. The cation contains an unusual and near planar $[Fe_6O_6]^{6+}$ six-rung ladder core of idealized C_2 symmetry (Fig. 4). Dissection of the structure shows that it can be considered as comprising three $[Fe_2O_2(O_2CR)L]^+$ units joined together. Each unit contains a planar $[Fe_2(\mu\text{-}O)_2]$ core with a $\mu\text{-}RCO_2^-$ bridging across one side of this and the L group bridging across the other side. The three units are linked by four inter-unit Fe–O bonds formed by a $\mu\text{-}O^{2-}$ ion on one unit attaching to an Fe^{III} on an adjacent unit. This is shown below, where the inter-unit bonds are indicated as dashed lines. Thus, four oxides are μ_3 while O7 and O12 at the ends remain μ. The chain of Fe_2 units is terminated by H_2O molecules O13 and O14. The units are arranged in an above–below–above fashion with respect to the L position about the Fe_6 plane.

The $[Fe_6O_6(H_2O)_2]$ core of complex **6** is shown in Fig. 5. Although the core can be described as approximately planar,

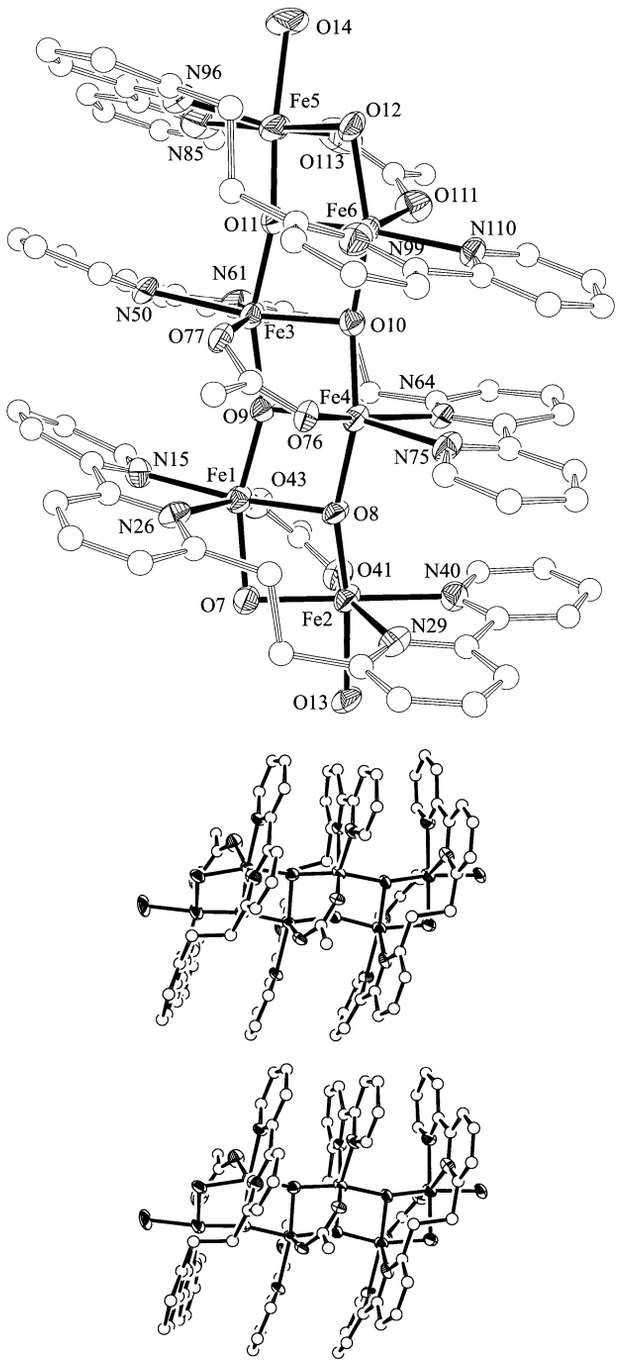

Fig. 4 ORTEP representation at the 50% probability level and stereopair of the $[Fe_6O_6(O_2CPh)_3L_3(H_2O)_2]^{3+}$ cation of complex **6**.

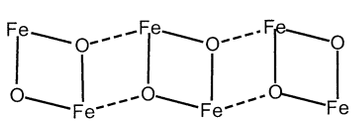

there is an observable degree of twist with deviations from the least-squares plane of 0.44 and 0.43 Å by atoms O7 and O12, respectively, and −0.69 and −0.52 Å by water atoms O13 and O14, respectively. The μ_3-oxide atoms are in a T-shaped geometry, with Fe–O–Fe angles in the range of 154.89 to 162.95°. The average Fe · · · Fe distance within a $[Fe_2O_2]^{2+}$ unit is 2.930 Å, with a slightly longer Fe · · · Fe distance of 3.005 Å between units. This feature correlates with a modest lengthening of the four inter-unit Fe–O^{2-} bonds (average 1.93 Å) compared with the four intra-unit Fe–O^{2-} bonds (average 1.87 Å).

A similar but shorter core structure is present in the cation of $[Fe_6O_4Cl_4(O_2CPh)_4(L)_2][FeCl_4]_2$, which contains only two linked

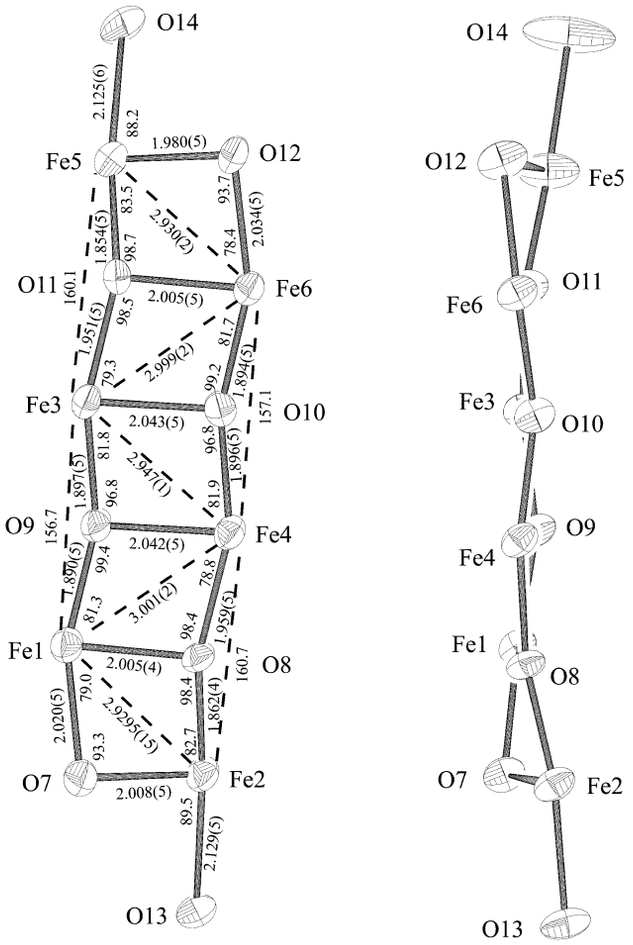

Fig. 5 The $[Fe_6O_6(H_2O)_2]$ core of the cation of complex **6** from two viewpoints emphasizing its near planar, six-rung ladder structure.

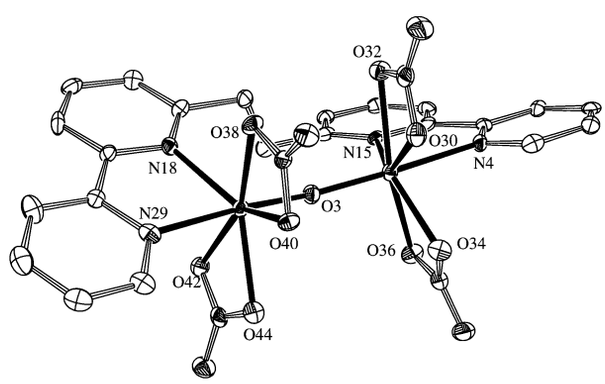

Fig. 6 ORTEP representation at the 50% probability level of $[Fe_2O(NO_3)_4L]$ **7**.

$[Fe_2O_2(O_2CR)L]^+$ units, as shown earlier. In this case the ladder is terminated with $[FeCl_2(O_2CPh)]$ caps instead of water molecules. No twist is seen in the planar core. No other similar planar core exists in iron chemistry, although a manganese cluster $[Mn_6O_2(OMe)_6(O_2CMe)_2(L'')_2]$ (L″ is a pentadentate Schiff-base ligand)[19] has an arrangement of Mn_6 similar to the arrangement of Fe_6 in the core of $[Fe_6O_4Cl_4(O_2CPh)_4L_2][FeCl_4]_2$.

Complex **7** crystallizes in monoclinic space group $P2_1/c$. The neutral molecule contains the same $[Fe_2O]^{4+}$ core seen in dinuclear complexes **2** and **5** with L contributing the only additional bridge (Fig. 6). Each Fe^{III} is seven-coordinate, with chelating NO_3^- ligands completing the coordination. The Fe · · · Fe distance in complex **7** of 3.4817(14) Å, while longer than in the carboxylate-containing complexes **2** and **5**, is shorter than in its direct bpy analog $[Fe_2O(NO_3)_4(bpy)_2]$ (3.5510(7) Å)[20]

Table 5 Selected bond diatances (Å) and angles (°) for $[Fe_6O_6(O_2CPh)_3L_3(H_2O)_2]Cl_3$ **6**

Fe(1)···Fe(2)	2.9295(15)	Fe(3)–N(61)	2.223(6)	Fe(2)–O(8)	1.862(4)	Fe(5)–O(113)	2.048(7)
Fe(3)···Fe(4)	2.9471(14)	Fe(4)–O(8)	1.959(5)	Fe(2)–O(13)	2.129(5)	Fe(5)–N(85)	2.152(8)
Fe(5)···Fe(6)	2.9301(16)	Fe(4)–O(9)	2.042(5)	Fe(2)–O(41)	2.032(5)	Fe(5)–N(96)	2.187(9)
Fe(1)–O(7)	2.020(5)	Fe(4)–O(10)	1.896(5)	Fe(2)–N(29)	2.205(6)	Fe(6)–O(10)	1.894(5)
Fe(1)–O(8)	2.005(4)	Fe(4)–O(76)	2.065(5)	Fe(2)–N(40)	2.176(6)	Fe(6)–O(11)	2.005(5)
Fe(1)–O(9)	1.890(5)	Fe(4)–N(64)	2.230(6)	Fe(3)–O(9)	1.897(5)	Fe(6)–O(12)	2.034(5)
Fe(1)–O(43)	2.058(5)	Fe(4)–N(75)	2.156(6)	Fe(3)–O(10)	2.043(5)	Fe(6)–O(111)	2.035(6)
Fe(1)–N(15)	2.147(6)	Fe(5)–O(11)	1.854(5)	Fe(3)–O(11)	1.951(5)	Fe(6)–N(99)	2.216(6)
Fe(1)–N(26)	2.236(6)	Fe(5)–O(12)	1.980(5)	Fe(3)–O(78)	2.071(5)	Fe(6)–N(110)	2.156(6)
Fe(2)–O(7)	2.008(5)	Fe(5)–O(14)	2.125(6)	Fe(3)–N(50)	2.178(6)		
O(7)–Fe(1)–O(8)	79.00(19)	O(7)–Fe(1)–O(9)	160.26(19)	O(9)–Fe(4)–O(10)	81.87(19)	O(113)–Fe(5)–N(96)	158.1(3)
O(7)–Fe(1)–O(43)	86.11(20)	O(13)–Fe(2)–N(29)	82.56(22)	O(9)–Fe(4)–O(76)	88.44(19)	N(85)–Fe(5)–N(96)	75.6(4)
O(7)–Fe(1)–N(15)	108.32(21)	O(13)–Fe(2)–N(40)	88.56(21)	O(9)–Fe(4)–N(64)	114.86(21)	O(10)–Fe(6)–O(11)	81.66(19)
O(7)–Fe(1)–N(26)	85.47(20)	O(41)–Fe(2)–N(29)	158.50(22)	O(9)–Fe(4)–N(75)	167.57(23)	O(10)–Fe(6)–O(12)	160.10(19)
O(8)–Fe(1)–O(9)	81.31(19)	O(41)–Fe(2)–N(40)	84.86(23)	O(10)–Fe(4)–O(76)	88.92(20)	O(10)–Fe(6)–O(111)	94.78(22)
O(8)–Fe(1)–O(43)	95.90(19)	N(29)–Fe(2)–N(40)	75.64(24)	O(10)–Fe(4)–N(64)	89.89(21)	O(10)–Fe(6)–N(99)	98.70(22)
O(8)–Fe(1)–N(15)	172.56(21)	O(9)–Fe(3)–O(10)	81.83(19)	O(10)–Fe(4)–N(75)	107.27(21)	O(10)–Fe(6)–N(110)	92.67(21)
O(8)–Fe(1)–N(26)	105.21(21)	O(9)–Fe(3)–O(11)	160.45(19)	O(76)–Fe(4)–N(64)	156.24(20)	O(11)–Fe(6)–O(12)	78.45(19)
O(9)–Fe(1)–O(43)	94.66(21)	O(9)–Fe(3)–O(78)	88.03(20)	O(76)–Fe(4)–N(75)	83.42(21)	O(11)–Fe(6)–O(111)	94.32(23)
O(9)–Fe(1)–N(15)	91.40(21)	O(9)–Fe(3)–N(50)	109.07(22)	N(64)–Fe(4)–N(75)	74.31(23)	O(11)–Fe(6)–N(99)	106.01(22)
O(9)–Fe(1)–N(26)	101.02(21)	O(9)–Fe(3)–N(61)	88.88(22)	O(11)–Fe(5)–O(12)	83.50(20)	O(11)–Fe(6)–N(110)	174.33(21)
O(43)–Fe(1)–N(15)	86.12(22)	O(10)–Fe(3)–O(11)	79.34(19)	O(11)–Fe(5)–O(14)	171.72(24)	O(12)–Fe(6)–O(111)	86.14(22)
O(43)–Fe(1)–N(26)	155.28(22)	O(10)–Fe(3)–O(78)	90.05(19)	O(11)–Fe(5)–O(113)	94.93(25)	O(12)–Fe(6)–N(99)	87.44(22)
N(15)–Fe(1)–N(26)	74.60(23)	O(10)–Fe(3)–N(50)	167.31(22)	O(11)–Fe(5)–N(85)	100.67(26)	O(12)–Fe(6)–N(110)	107.22(21)
O(7)–Fe(2)–O(8)	82.75(20)	O(10)–Fe(3)–N(61)	113.64(22)	O(11)–Fe(5)–N(96)	98.34(26)	O(111)–Fe(6)–N(99)	156.97(24)
O(7)–Fe(2)–O(13)	89.54(19)	O(11)–Fe(3)–O(78)	97.14(20)	O(12)–Fe(5)–O(14)	88.22(23)	O(111)–Fe(6)–N(110)	86.20(24)
O(7)–Fe(2)–O(41)	88.28(20)	O(11)–Fe(3)–N(50)	90.25(21)	O(12)–Fe(5)–O(113)	90.83(24)	N(99)–Fe(6)–N(110)	74.64(24)
O(7)–Fe(2)–N(29)	110.86(23)	O(11)–Fe(3)–N(61)	93.87(22)	O(12)–Fe(5)–N(85)	174.3(3)	Fe(1)–O(7)–Fe(2)	93.32(20)
O(7)–Fe(2)–N(40)	172.93(23)	O(78)–Fe(3)–N(50)	84.00(22)	O(12)–Fe(5)–N(96)	107.8(3)	Fe(1)–O(8)–Fe(2)	98.41(21)
O(8)–Fe(2)–O(13)	170.02(21)	O(78)–Fe(3)–N(61)	155.40(22)	O(14)–Fe(5)–O(113)	85.3(3)	Fe(1)–O(8)–Fe(4)	98.37(19)
O(8)–Fe(2)–O(41)	97.98(20)	N(50)–Fe(3)–N(61)	73.99(25)	O(14)–Fe(5)–N(85)	87.6(3)	Fe(2)–O(8)–Fe(4)	160.69(27)
O(8)–Fe(2)–N(29)	94.24(21)	O(8)–Fe(4)–O(9)	78.77(18)	Fe(1)–O(9)–Fe(3)	156.7(3)	Fe(4)–O(10)–Fe(6)	157.07(27)
O(8)–Fe(2)–N(40)	99.84(22)	O(8)–Fe(4)–O(10)	159.24(19)	Fe(1)–O(9)–Fe(4)	99.39(20)	Fe(3)–O(11)–Fe(5)	160.12(28)
O(13)–Fe(2)–O(41)	88.07(20)	O(8)–Fe(4)–O(76)	97.93(19)	Fe(3)–O(9)–Fe(4)	96.79(20)	Fe(3)–O(11)–Fe(6)	98.54(20)
O(8)–Fe(4)–N(64)	91.49(20)	O(14)–Fe(5)–N(96)	84.0(3)	Fe(3)–O(10)–Fe(4)	96.79(21)	Fe(5)–O(11)–Fe(6)	98.72(21)
O(8)–Fe(4)–N(75)	93.02(21)	O(113)–Fe(5)–N(85)	85.0(4)	Fe(3)–O(10)–Fe(6)	99.16(21)	Fe(5)–O(12)–Fe(6)	93.73(21)

Table 6 Selected bond distances (Å) and angles (°) for $[Fe_2O(NO_3)_4L]$ **7**

Fe(1)···Fe(2)	3.4817(14)	Fe(2)–O(3)	1.770(4)
Fe(1)–O(3)	1.779(4)	Fe(2)–O(38)	2.181(4)
Fe(1)–O(30)	2.182(4)	Fe(2)–O(40)	2.150(4)
Fe(1)–O(32)	2.239(4)	Fe(2)–O(42)	2.221(4)
Fe(1)–O(34)	2.167(4)	Fe(2)–O(44)	2.210(4)
Fe(1)–O(36)	2.223(4)	Fe(2)–N(18)	2.190(5)
Fe(1)–N(4)	2.124(4)	Fe(2)–N(29)	2.143(5)
Fe(1)–N(15)	2.217(5)		
O(3)–Fe(1)–O(30)	96.17(16)	O(32)–Fe(1)–O(36)	159.96(15)
O(3)–Fe(1)–O(32)	97.24(16)	O(32)–Fe(1)–N(4)	81.78(16)
O(3)–Fe(1)–O(34)	97.29(17)	O(32)–Fe(1)–N(15)	81.72(16)
O(3)–Fe(1)–O(36)	95.87(16)	O(34)–Fe(1)–O(36)	58.89(14)
O(3)–Fe(1)–N(4)	176.95(18)	O(34)–Fe(1)–N(4)	85.42(16)
O(3)–Fe(1)–N(15)	100.79(17)	O(34)–Fe(1)–N(15)	137.36(16)
O(30)–Fe(1)–O(32)	58.10(15)	O(36)–Fe(1)–N(4)	84.34(17)
O(30)–Fe(1)–O(34)	76.74(16)	O(36)–Fe(1)–N(15)	80.98(16)
O(30)–Fe(1)–O(36)	135.10(15)	N(4)–Fe(1)–N(15)	76.23(17)
O(30)–Fe(1)–N(4)	85.78(16)	O(3)–Fe(2)–O(38)	95.52(16)
O(30)–Fe(1)–N(15)	138.03(17)	O(3)–Fe(2)–O(40)	96.57(16)
O(32)–Fe(1)–O(34)	133.68(15)	O(3)–Fe(2)–O(42)	93.23(16)
O(3)–Fe(2)–O(44)	93.75(16)	O(40)–Fe(2)–N(18)	137.11(17)
O(3)–Fe(2)–N(18)	105.16(18)	O(40)–Fe(2)–N(29)	85.14(16)
O(3)–Fe(2)–N(29)	175.27(18)	O(42)–Fe(2)–O(44)	58.11(14)
O(38)–Fe(2)–O(40)	59.81(14)	O(42)–Fe(2)–N(18)	78.32(16)
O(38)–Fe(2)–O(42)	159.35(15)	O(42)–Fe(2)–N(29)	82.58(16)
O(38)–Fe(2)–O(44)	139.47(15)	O(44)–Fe(2)–N(18)	133.41(16)
O(38)–Fe(2)–N(18)	81.35(16)	O(44)–Fe(2)–N(29)	82.18(16)
O(38)–Fe(2)–N(29)	89.15(17)	N(18)–Fe(2)–N(29)	76.22(18)
O(40)–Fe(2)–O(42)	137.47(15)	Fe(1)–O(3)–Fe(2)	157.60(23)
O(40)–Fe(2)–O(44)	79.97(15)		

or even in the carboxylate-bridged $[Fe_2O(O_2CMe)L'_2]ClO_4$ (3.564 Å).[18]

The crystal structures of complexes **8** and **9** have not been obtained, but their structures can readily be deduced from their formulations, the structure of **7**, and previously reported species with L or bpy groups. The $[Fe_2OCl_6L]^{2-}$ anion of **8** likely has the structure depicted, which is the same as **7** except

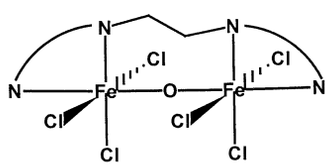

anion of **8**

that chelating NO_3^- groups are replaced by terminal Cl^- ions, and the Fe^{III} are thus six- rather than seven-coordinate. In contrast, the $[Fe_2OCl_2L_2]^{2+}$ cation of **9** has two L groups and

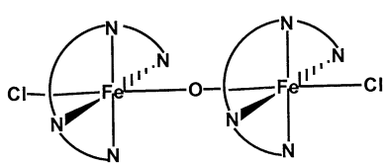

cation of **9**

thus the latter cannot both be bridging. In fact, the structure is very likely that shown, with the L groups each chelating to a single Fe^{III}; this mode for L has previously been observed in $[CuL]^{2+}$ containing a square-planar Cu^{II}.[4] More importantly, the corresponding vanadium(III) complex $[V_2OCl_2L_2]^{2+}$ is known[21] and has been shown crystallographically to have exactly the structure proposed for **9**.

Magnetic susceptibility studies

Solid-state, variable-temperature magnetic susceptibility (χ_m) studies were carried out on powder samples of complexes

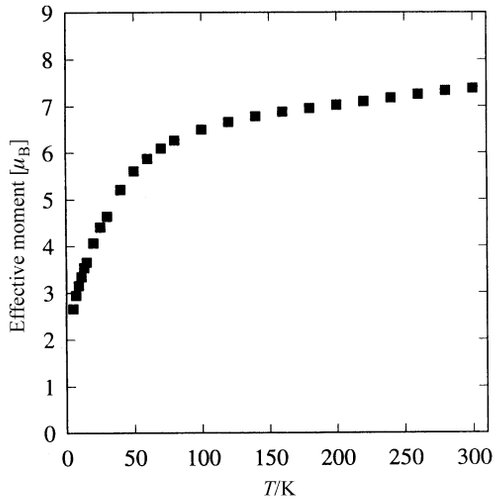

Fig. 7 Plot of effective magnetic moment (μ_{eff} *vs.* T) for complex **4**·2MeCN. The solid line is a fit of the 15.0–300 K data by the appropriate theoretical equation; see the text for the fitting parameters.

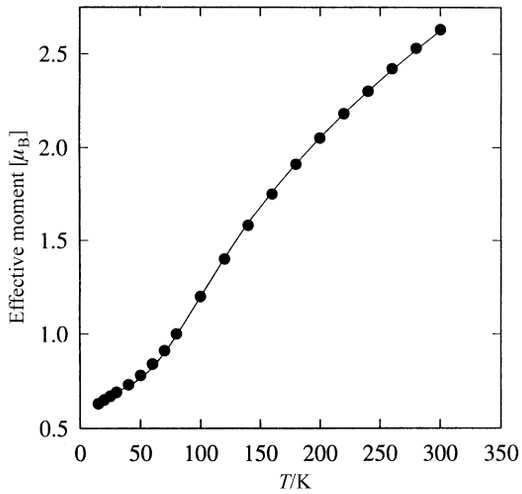

Fig. 8 Plot of effective magnetic moment (μ_{eff}) *vs.* T for complex **6**·6H_2O.

4·2MeCN and **6**·6H_2O in the temperature range 5.00 to 300 K and in an applied field of 10.0 kG (1 Tesla).

For complex **4** the effective magnetic moment (μ_{eff}) and $\chi_m T$ values per Fe_2 decrease from 2.63 μ_B and 0.87 cm^3 K mol^{-1}, respectively, at 300 K to 0.54 μ_B and 0.04 cm^3 K mol^{-1} at 5.00 K (Fig. 7). The 300 K values are considerably less than the 8.37 μ_B and 8.754 cm^3 K mol^{-1} expected for a dinuclear species containing non-interacting Fe^{III} ($S = 5/2$) ions, suggesting the presence of a relatively strong antiferromagnetic exchange interaction in **4**. The μ_{eff} *vs.* T data in the 15.0–300 K range were fitted by the theoretical equation derived for a Heisenberg exchange model ($H = -2JS_1S_2$) with $S_1 = S_2 = 5/2$ and including the contribution for a variable amount of $S = 5/2$ paramagnetic impurity. The χ_m *vs.* T equation for an exchange-coupled Fe^{III}_2 system is given elsewhere;[22] converting it into μ_{eff} and incorporating the contribution of a $S = 5/2$ impurity (molar fraction p) gives eqn. (8), where χ_m also contains the contribution from

$$\mu_{eff} = 2.828[(1 - p)\chi_m T + 4.38p]^{1/2} \quad (8)$$

temperature-independent paramagnetism (TIP). This equation was used to fit the experimental μ_{eff} *vs.* T data, and the obtained fitting parameters were $J = -119(1)$ cm^{-1}, $g = 1.96(2)$ and $p = 0.0102(2)$, with TIP held constant at 500×10^{-6} cm^3 mol^{-1}. This fit is shown as a solid line in Fig. 7. The complex is thus antiferromagnetically coupled with a $S = 0$ ground state and a $S = 1$ first excited state at 238 cm^{-1} above the ground state.

The J value for complex **4** is as expected from the empirical J *vs.* P relationship reported by Gorun and Lippard,[14] where P is defined as half the shortest superexchange pathway between the two Fe^{III}. The J *vs.* P relationship is described by eqn. (9),

$$-J = A \exp(BP) \quad (9)$$

where $A = 8.763 \times 10^{10}$, $B = -12.663$, and J is based on the $H = -2JS_iS_j$ spin Hamiltonian. For **4**, half the Fe(1)–O(3)–Fe(2) pathway distance is 1.777(6) Å, giving a predicted J of $-148(11)$ cm^{-1}. The experimental value of -119 cm^{-1} is significantly weaker; however, we note that the complex [Fe_2O(mpdp)(4,4′-Me_2bpy)$_2Cl_2$] has a similar P of 1.773(3) Å, a predicted J of 156(6) cm^{-1}, and an experimental value of -119 cm^{-1}, the same as for **4**.[16]

For complex **6** the μ_{eff} ($\chi_m T$) values decrease slowly from 7.38 μ_B (6.81 cm^3 K mol^{-1}) at 300 K to 6.66 μ_B (5.54 cm^3 K mol^{-1}) at 120 K, then rapidly decrease to 2.65 μ_B (0.878 cm^3 K mol^{-1}) at 5.00 K (Fig. 8). The 300 K values are considerably less than expected for six non-interacting Fe^{III} (14.5 μ_B and 35 cm^3 K mol^{-1}) indicating antiferromagnetic exchange interactions, and the rapidly decreasing shape of the curve at the lowest temperatures is strongly suggestive of a $S = 0$ ground state. This behavior is very similar to that of previously reported [Fe_6O_4-Cl_4(O_2CPh)$_4$L$_2$]$^{2+}$, which has a four-rung ladder structure and a $S = 0$ ground state.[7]

The $S = 0$ ground state of the Fe_6 cation of complex **6** is not unexpected given that this is the most common ground state for Fe^{III}_x clusters where x is an even number. Some important exceptions, however, include [Fe_8O_2(OH)$_{12}$(tacn)$_6$]$^{8+}$ ($S = 10$),[24] [Fe_4(OMe)$_6$(dpm)$_6$] ($S = 5$, dpm$^-$ is the anion of dibenzoylmethane)[24] and [Fe_6O_2(OH)$_2$(O_2CMe)$_{10}$(hmp)$_2$] ($S = 5$; hmp is the anion of 2-(hydroxymethyl)pyridine);[25] in these cases the non-zero ground state can be rationalized by the Fe_x topology which introduces competing antiferromagnetic exchange interactions and resultant spin frustration effects which prevent equal amounts of parallel (spin-up) and antiparallel (spin-down) spin. For the extended ladder-like topology of the cation of **6**, however, this is not expected: the [Fe_2O_2] unit is expected to be strongly antiferromagnetically coupled, and since the Fe_6 ladder can be considered as five edge-fused [Fe_2O_2] units, then the ground state spin alignments are likely to be as shown, giving the experimentally observed $S = 0$ ground state. The depicted alignment assumes that the exchange interactions between iron(III) pairs bridged by a single O^{2-} ion (*i.e.*, the [Fe_2O] pairs) are weaker than those between pairs bridged by two O^{2-} ions (*i.e.*, the [Fe_2O_2] pairs), because both types of interaction are expected to be antiferromagnetic. This is reasonable given that oxide bridges are excellent mediators of exchange interactions. Unfortunately, the complexity of the Fe_6 topology of **6**, which involves five non-equivalent J values, precludes determination of the individual exchange parameters.

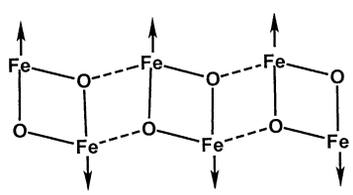

Conclusions

The use of the bis-bipyridyl ligand L in iron(III) carboxylate chemistry continues to provide access to interesting supramolecular assemblies of dinuclear units. In the present work a number of discrete dinuclear species have been isolated, together with an example where three dinuclear units are linked to produce a six-rung ladder-like [Fe_6O_6] core. This fulfils the

prediction in a previous report[7] where we described the four-rung ladder-like $[Fe_4O_4]$ core of $[Fe_6O_4Cl_4(O_2CPh)_4L_2]^{2+}$ and stated that there appeared no reason why longer assemblies should not be made. Indeed, the Fe_6O_6 core of **6** is merely the member with $n = 3$ of the $[Fe_{2n}O_{2n}]$ family of ladder-like cores, and longer units should also be accessible.

In most cases to date the L ligand both chelates and bridges an Fe_2 pair and thus acts as a binucleating group. Consideration of the conformation of free **1**, and the structures of **2**, **5** and **6**, suggests that L has a conformational preference for bridging above a planar $[M_2(\mu\text{-}X)_2]$ rhomb as found in, *e.g.*, **6**, and previously reported $[Fe_2(OMe)_2Cl_2(O_2CPh)L]^+$[7] and $[Co_8O_4(OH)_4(O_2CMe)_6L_2]^{2+}$.[5] Similarly, the $[Fe_2(\mu\text{-}O)(\mu\text{-}O_2CPh)]^{3+}$ core of **5** allows L to bridge with little strain, whereas the $[Fe_2(\mu\text{-}O)(\mu\text{-}O_2CPh)_2]^{2+}$ core of **2** causes L to adopt a much more strained conformation. Both the present and previous results thus suggest the possibility of synthesizing further novel examples of complexes that contain $[M_2O_2]$ units bridged/chelated by ligand L, and this is currently under exploration.

Acknowledgements

This work was supported by National Science Foundation grants to G. C. and D. N. H.

References

1 G. Aromí, S. M. J. Aubin, M. A. Bolcar, G. Christou, H. J. Eppley, K. Folting, D. N. Hendrickson, J. C. Huffman, R. C. Squire, H.-L. Tsai, S. Wang and M. W. Wemple, *Polyhedron*, 1998, **17**, 3005; G. Aromí, J.-P. Claude, M. J. Knapp, J. C. Huffman, D. N. Hendrickson and G. Christou, *J. Am. Chem. Soc.*, 1998, **120**, 2977; M. W. Wemple, D. K. Coggin, J. B. Vincent, J. K. McCusker, W. E. Streib, J. C. Huffman, D. N. Hendrickson and G. Christou, *J. Chem. Soc.*, *Dalton Trans.*, 1998, 719; H. J. Eppley, N. de Vries, S. Wang, S. M. J. Aubin, H.-L. Tsai, K. Folting, D. N. Hendrickson and G. Christou, *Inorg. Chim. Acta*, 1997, **263**, 323; H. J. Eppley, S. M. J. Aubin, W. E. Streib, J. C. Bollinger, D. N. Hendrickson and G. Christou, *Inorg. Chem.*, 1997, **36**, 109; J. B. Vincent, H.-L. Tsai, A. G. Blackman, S. Wang, P. D. W. Boyd, K. Folting, J. C. Huffman, E. B. Lobkovsky, D. N. Hendrickson and G. Christou, *J. Am. Chem. Soc.*, 1993, **115**, 12353; S. Wang, H.-L. Tsai, W. E. Streib, G. Christou and D. N. Hendrickson, *J. Chem. Soc.*, *Chem. Commun.*, 1992, 677; S. Wang, J. C. Huffman, K. Folting, W. E. Streib, E. B. Lobkovsky and G. Christou, *Angew. Chem.*, *Int. Ed. Engl.*, 1991, **30**, 1672.

2 J. B. Vincent, C. Christmas, H.-R. Chang, Q. Li, P. D. W. Boyd, J. C. Huffman, D. N. Hendrickson and G. Christou, *J. Am. Chem. Soc.*, 1989, **111**, 2086.

3 S. Ferrere and C. M. Elliott, *Inorg. Chem.*, 1995, **34**, 5818; M.-T. Youinou, R. Ziessel and J.-M. Lehn, *Inorg. Chem.*, 1991, **30**, 2144; C. Piguet, G. Bernardinelli and G. Hopfgartner, *Chem. Rev.*, 1997, **97**, 2005; B. Hasenknopf, J.-M. Lehn, N. Boumediene, A. Dupont-Gervais, A. Van Dorsselaer, B. Kneisel and D. Fenske, *J. Am. Chem. Soc.*, 1997, **119**, 10956; P. N. W. Baxter, J.-M. Lehn and K. Rissanen, *Chem. Commun.*, 1997, 1323; P. L. Jones, K. J. Byrom, J. C. Jeffery, J. A. McCleverty and M. D. Ward, *Chem. Commun.*, 1997, 1361; H. Sleiman, P. N. W. Baxter, J.-M. Lehn, K. Airola and K. Rissanen, *Inorg. Chem.*, 1997, **36**, 4734; P. N. W. Baxter, J.-M. Lehn, J. Fischer and M.-T. Youinou, *Angew. Chem.*, *Int. Ed. Engl.*, 1994, **33**, 2284; P. Baxter, J.-M. Lehn, A. De Cian and J. Fischer, *Angew. Chem.*, *Int. Ed. Engl.*, 1993, **32**, 69; E. C. Constable, *Chem. Commun.*, 1997, 1073.

4 T. Garber, S. Van Wallendael, D. P. Rillema, M. Kirk, W. E. Hatfield, J. H. Welch and P. Singh, *Inorg. Chem.*, 1990, **29**, 2863.

5 V. A. Grillo, Z. Sun, K. Folting, D. N. Hendrickson and G. Christou, *Chem. Commun.*, 1996, 223.

6 V. A. Grillo, M. J. Knapp, J. C. Bollinger, D. N. Hendrickson and G. Christou, *Angew. Chem.*, *Int. Ed. Engl.*, 1996, **35**, 1818.

7 C. M. Grant, M. J. Knapp, W. E. Streib, J. C. Huffman, D. N. Hendrickson and G. Christou, *Inorg. Chem.*, 1998, **37**, 6065.

8 W. H. Armstrong and S. J. Lippard, *Inorg. Chem.*, 1985, **24**, 981.

9 (*a*) P. Main, S. J. Fiske, S. E. Hill, L. Lessinger, G. Germain, J.-P. Declerq and M. M. Woolfson, MULTAN 78, Universities of York and Louvain, 1978; (*b*) G. M. Sheldrick, *SHELXTL/PC Users Manual*, Siemens Analytical X-Ray Instruments, Inc., Madison, WI, 1990; (*c*) J. de Meulenaer and H. Tompa, *Acta Crystallogr.*, 1965, **19**, 1014; (*d*) C. K. Johnson, ORTEP II, Report ORNL-5138, Oak Ridge National Laboratory, Oak Ridge, TN, 1976.

10 E. C. Constable, S. M. Elder, J. V. Walker, P. D. Wood and D. A. Tocher, *J. Chem. Soc.*, *Chem. Commun.*, 1992, 229.

11 A. Hergold-Brundić, Z. Popović and D. Matković-Čalogović, *Acta Crystallogr.*, *Sect. C*, 1996, **52**, 3154.

12 M. H. Chisholm, J. C. Huffman, I. P. Rothwell, P. G. Bradley, N. Kress and W. H. Woodruff, *J. Am. Chem. Soc.*, 1981, **103**, 4945; E. C. Constable, S. M. Elder, J. Healy and D. A. Tocher, *J. Chem. Soc.*, *Dalton Trans.*, 1990, 1669; C. A. Bessel, R. F. See, D. L. Jameson, M. W. Churchill and K. J. Takeuchi, *J. Chem. Soc.*, *Dalton Trans.*, 1992, 3223; F. Vögtle, M. Frank, M. Nieger, P. Belser, A. von Zelewsky, V. Balzani, F. Barigelletti, L. De Cola and L. Flamigni, *Angew. Chem.*, *Int. Ed. Engl.*, 1993, **32**, 1643; C. Kaes, M. W. Hosseini, R. Ruppert, A. De Cian and J. Fischer, *J. Chem. Soc.*, *Chem. Commun.*, 1995, 1445; F. R. Heirtzler, M. Neuburger, M. Zehnder and E. C. Constable, *Liebigs Ann./Recueil*, 1997, 297.

13 B. Milani, A. Anzilutti, L. Vicentini, A. Sessanta o Santi, E. Zangrando, S. Geremia and G. Mestroni, *Organometallics*, 1997, **16**, 5064; P. K. Bakshi, T. S. Cameron and O. Knop, *Can. J. Chem.*, 1996, **74**, 201.

14 S. M. Gorun and S. J. Lippard, *Inorg. Chem.*, 1991, **30**, 1625.

15 J. B. Vincent, J. C. Huffman, G. Christou, Q. Li, M. A. Nanny, D. N. Hendrickson, R. H. Fong and R. H. Fish, *J. Am. Chem. Soc.*, 1988, **110**, 6898.

16 R. H. Beer, W. B. Tolman, S. G. Bott and S. J. Lippard, *Inorg. Chem.*, 1991, **30**, 2082.

17 J. Wang, M. S. Mashuta, Z. Sun, J. F. Richardson, D. N. Hendrickson and R. M. Buchanan, *Inorg. Chem.*, 1996, **35**, 6642; S. K. Mandal and L. Que, Jr., *Inorg. Chem.*, 1997, **36**, 5424; B. Graham, B. Moubaraki, K. S. Murray, L. Spiccia, J. D. Cashion and D. C. R. Hockless, *J. Chem. Soc.*, *Dalton Trans.*, 1997, 887; T. Okuno, S. Ito, S. Ohba and Y. Nishida, *J. Chem. Soc.*, *Dalton Trans.*, 1997, 3547.

18 A. Hazell, K. B. Jensen, C. J. McKenzie and H. Toftlund, *J. Chem. Soc.*, *Dalton Trans.*, 1993, 3249.

19 X. Xia, M. Verelst, J.-C. Daran and J.-P. Tuchagues, *J. Chem. Soc.*, *Chem. Commun.*, 1995, 2155.

20 K. L. Taft, A. Masschelein, S. Liu, S. J. Lippard, D. Garfinkel-Shweky and A. Bino, *Inorg. Chim. Acta*, 1992, **198**–**200**, 627; H. Matsushima, K. Iwasawa, K. Ide, Md. Yeamin Reza, M. Koikawa and T. Tokii, *Inorg. Chim. Acta*, 1998, **274**, 224.

21 C. M. Grant, B. J. Stamper, M. P. Knapp, K. Folting, J. C. Huffman, D. N. Hendrickson and G. Christou, *J. Chem. Soc.*, *Dalton Trans.*, 1999, 3399.

22 C. J. O'Connor, *Prog. Inorg. Chem.*, 1982, **29**, 203.

23 C. Delfs, D. Gatteschi, L. Pardi, R. Sessoli, K. Wieghardt and D. Hanke, *Inorg. Chem.*, 1993, **32**, 3099.

24 A. L. Barra, A. Caneschi, A. Cornia, F. Fabrizi de Biani, D. Gatteschi, C. Sangregorio, R. Sessoli and L. Sorace, *J. Am. Chem. Soc.*, 1999, **121**, 5302.

25 C. A. Christmas, H.-L. Tsai, L. Pardi, J. M. Kesselman, P. K. Gantzel, R. K. Chadha, D. Gatteschi, D. F. Harvey and D. N. Hendrickson, *J. Am. Chem. Soc.*, 1993, **115**, 12483.